

# The hadronic contribution to the running of $\alpha$ and $\sin^2 \theta_W$

Marco Cè   Antoine Gérardin   Georg von Hippel   Ben Hörz  
Renwick J. Hudspith   Simon Kuberski   Harvey B. Meyer   Kohtaroh Miura  
Daniel Mohler   Konstantin Ottnad   Srijit Paul   Andreas Risch  
Teseo San José   Jonas Wilhelm   Hartmut Wittig

---

GDR-InF annual workshop 2022

*Domaine Lyon Saint-Joseph*

02-04 November 2022

---

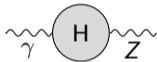
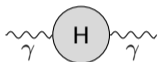


## Standard approach

Use the optical theorem and the  $R$ -ratio of experimental data

$$R(Q^2) \equiv \frac{\sigma_{\text{total}}(e^+e^- \rightarrow \text{hadrons})}{\sigma(e^+e^- \rightarrow \mu^+\mu^-)}$$

It gives access to the vacuum polarisation



With this diagram, we can compute the QCD contribution to several quantities:

$a_\mu$

$\alpha(Q^2)$

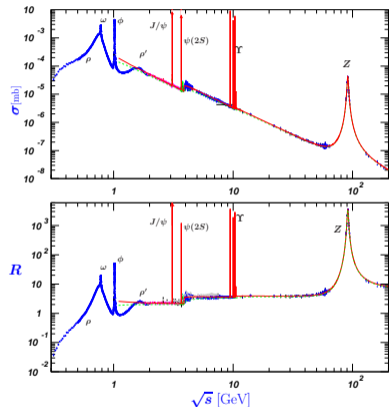
$\sin^2 \theta_W(Q^2)$

All are used in tests of the Standard Model

$\alpha(m_Z^2)$  enters the electroweak global fits  $\rightarrow m_H = 91_{-16}^{+18}$  GeV

[1]

$a_\mu$  and  $\alpha$  are connected



[2]

## The main equations

Start from the vacuum polarisation tensor

$$\Pi_{\mu\nu}^{ab}(Q) = \int d^4x e^{iQx} \langle V_\mu^a(x) V_\nu^b(0) \rangle_{\text{QCD}} = (Q_\mu Q_\nu - \eta_{\mu\nu} Q^2) \Pi^{ab}(Q^2)$$



Use the time-momentum representation [3, 4] to express the subtracted vacuum polarisation function (sVPF)

$$\bar{\Pi}^{ab}(-Q^2) = \int_0^\infty dt G^{ab}(t) K(t, Q^2)$$

$$G^{ab}(t) = -\frac{a^3}{3} \sum_{k=1}^3 \sum_{\bar{x}} \langle V_k^a(x) V_k^b(0) \rangle_{\text{QCD}}$$

Parametrise the running with the formulas

$$\alpha(-Q^2) = \frac{\alpha}{1 - \Delta\alpha(-Q^2)}$$

$$\sin^2 \theta_W(-Q^2) = \sin^2 \theta_W (1 + \Delta \sin^2 \theta_W(-Q^2))$$

Relate the leading hadronic contribution to the vacuum polarisation function (VPF):

$$(\Delta\alpha)_{\text{had}}(-Q^2) = 4\pi\alpha \bar{\Pi}^{\gamma\gamma}(-Q^2)$$

$$(\Delta \sin^2 \theta_W)_{\text{had}}(-Q^2) = -\frac{4\pi\alpha}{\sin^2 \theta_W} \bar{\Pi}^{Z\gamma}(-Q^2)$$

## The vector currents $V_k^\gamma$ , $V_k^Z$

- The two basic currents are

$$V_k^\gamma = \frac{2}{3}\bar{u}\gamma_k u - \frac{1}{3}\bar{d}\gamma_k d + \frac{2}{3}\bar{c}\gamma_k c - \frac{1}{3}\bar{s}\gamma_k s, \quad V_k^{T_3} = \frac{1}{4}\bar{u}\gamma_k u - \frac{1}{4}\bar{d}\gamma_k d + \frac{1}{4}\bar{c}\gamma_k c - \frac{1}{4}\bar{s}\gamma_k s$$

- An isospin decomposition is very convenient,

$$V_k^\gamma = V_k^3 + 1/\sqrt{3}V_k^8 + 2/3V_k^c$$

$$V_k^Z = V_k^{T_3} - \sin^2 \theta_W V_k^\gamma = (1/2 - \sin^2 \theta_W)V_k^\gamma - 1/6V_k^0 - 1/12V_k^c$$

- In terms of the quark flavours,

Iso-vector,	$V_k^3 = 1/2(\bar{u}\gamma_k u - \bar{d}\gamma_k d)$
Iso-scalar,	$V_k^8 = 1/(2\sqrt{3})(\bar{u}\gamma_k u + \bar{d}\gamma_k d - 2\bar{s}\gamma_k s)$
Iso-singlet,	$V_k^0 = 1/2(\bar{u}\gamma_k u + \bar{d}\gamma_k d + \bar{s}\gamma_k s)$

- We use two  $V_k$  discretisations: local and conserved

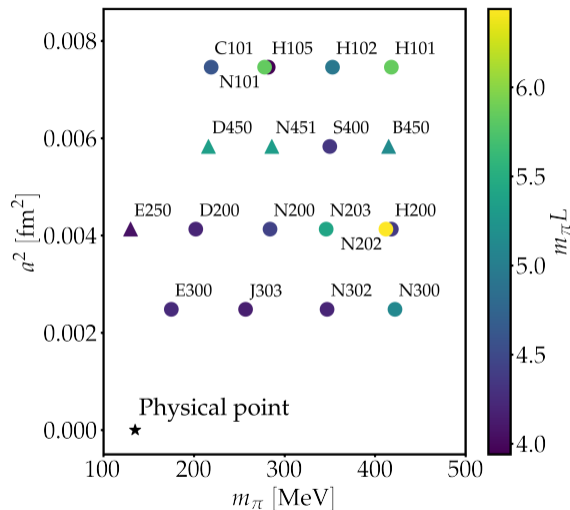
$$(V_k^a)^L = \bar{\psi}(x)\gamma_k \lambda^a / 2 \psi(x)$$

$$(V_k^a)^C = 1/2 \left( \bar{\psi}(x + a\hat{k})(1 + \gamma_k) U_k^\dagger(x) \lambda^a / 2 \psi(x) - \bar{\psi}(x)(1 - \gamma_k) U_k(x) \lambda^a / 2 \psi(x + a\hat{k}) \right)$$

## Coordinated lattice simulations (CLS)

- ▶  $N_f = 2 + 1$   $\mathcal{O}(a)$ -improved Wilson action
- ▶ Tree-level improved Lüscher-Weisz action
- ▶ Periodic/open temporal boundary conditions
- ▶ Chiral trajectory  $m_\pi^2/2 + m_K^2 \approx \text{const}$
- ▶ Pion masses  $130 \text{ MeV} < m_\pi < 420 \text{ MeV}$
- ▶  $a = (50, 64, 76 \text{ and } 86) \times 10^{-3} \text{ fm}$
- ▶ Volumes  $m_\pi L > 4$
- ▶ Local and conserved discretisations
- ▶ Use the scale  $\sqrt{8t_0}$  [5] or  $af_\pi$  [6]

$$-\left\langle \left( \begin{array}{c} \gamma_\mu \xrightarrow{f_1} \gamma_\nu \\ \gamma_\mu \xrightarrow{f_2} \gamma_\nu \end{array} \right) \right\rangle, \left\langle \left( \begin{array}{c} \gamma_\mu \xrightarrow{f_1} \gamma_\nu \\ \gamma_\nu \xrightarrow{f_2} \gamma_\mu \end{array} \right) \right\rangle$$



[7, 5]

## Sources of uncertainty

To produce highly accurate results, our analysis needs to study the following topics:

- Signal-to-noise ratio
- Finite box size
- Finite lattice spacing
- Unphysical quark masses
- Scale setting
- Isospin breaking effects (quark-connected component estimated in subset of ensembles)
- Missing sea charm and bottom quarks (insignificant [8, 9])

## Signal-to-noise ratio

Note  $G$ 's spectral representation

$$G(t) = \sum_n |A_n|^2 e^{-E_n t}$$

which implies the noise has also an spectral representation

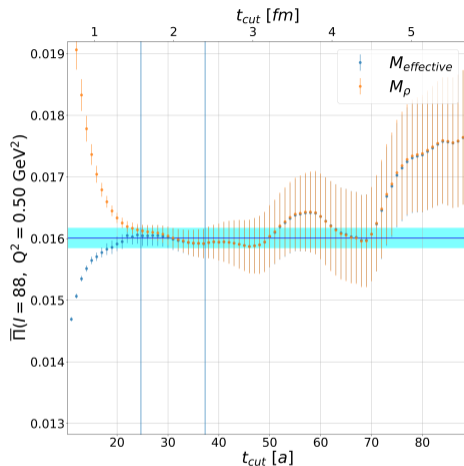
$$\sigma_G \equiv \sqrt{\langle (VV)^2 \rangle - \langle VV \rangle^2} = \sum_m |A'_m|^2 e^{-E'_m t}$$

**Problem:** Signal-to-noise ratio decays exponentially

$$\frac{G(t)}{\sigma_G} \sim e^{-\Delta t}$$

**Solution:** use the bounding method

$$0 \leq G(t_{\text{cut}}) e^{-m_{\text{eff}}(t)(t-t_{\text{cut}})} \leq G(t) \leq G(t_{\text{cut}}) e^{-E_0(t-t_{\text{cut}})}, \quad t \geq t_{\text{cut}} \quad [9]$$



## Finite box size

We use periodic boundary conditions in space → Particles go around the box → Estimate and remove this effect

Several pion isovector states affect the most

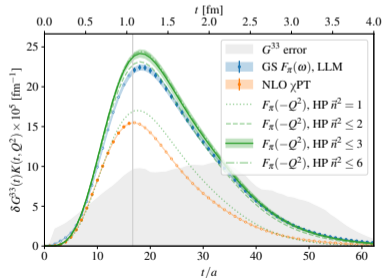
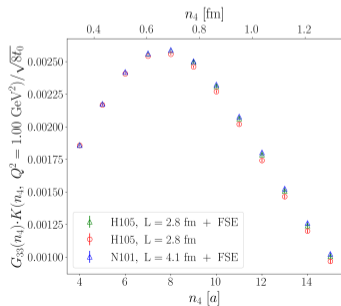
$$G^{33}(t, \infty) = G^{33}(t, L) + \Delta G^{33}(t, L)$$

$$\Delta G^{33}(t, L) = G_{\text{model}}^{33}(t, \infty) - G_{\text{model}}^{33}(t, L)$$

We use two methods to estimate  $\Delta G^{33}(t, L)$

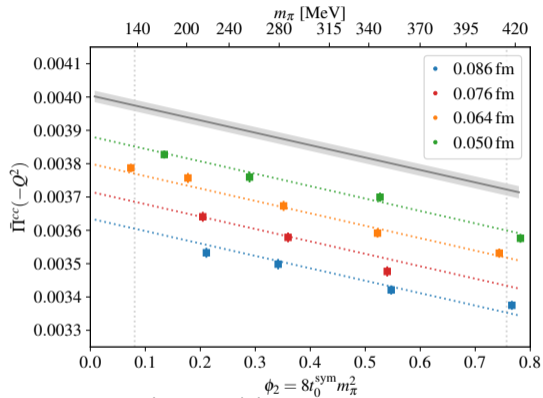
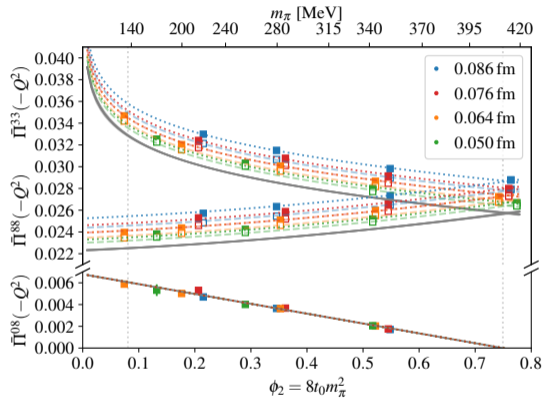
Hansen-Patella (HP) for many-pion states [10, 11]

Meyer-Lellouch-Lüscher (MLL) for two-pion states [12, 4, 13, 14]



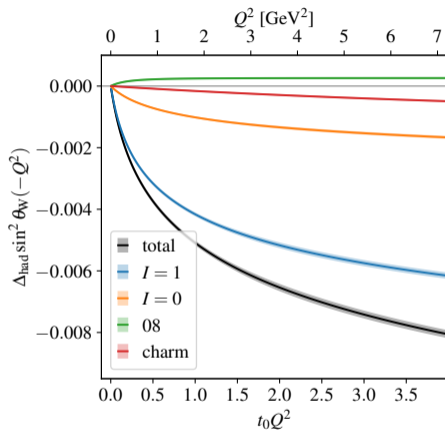
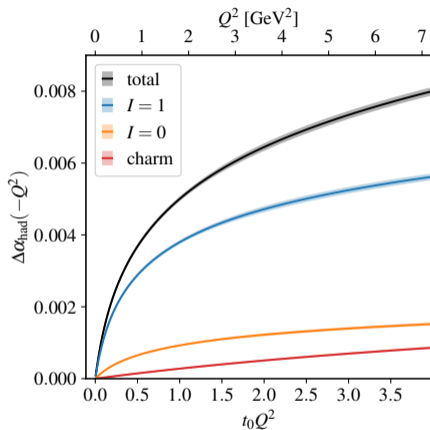


# Finite lattice spacing and unphysical quark masses



$(\Delta\alpha)_{\text{had}}(-1 \text{ GeV}^2) \times 10^6 = 3864$  (17) (8) (22) (4) (12) [32, 0.8%]  
 Statistical      Extrapolation      Isospin breaking      Total Percentage

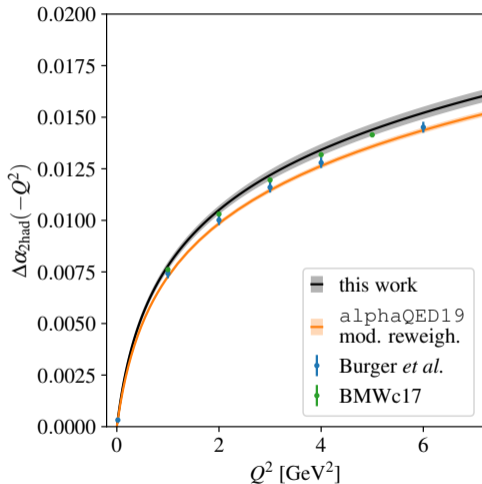
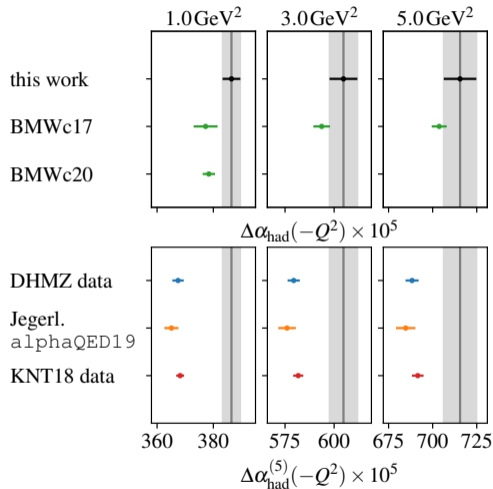
## Running with $Q^2$



Use Padé Ansätze for  $Q^2 \leq 7 \text{ GeV}^2$

$$(\Delta\alpha)_{\text{had}}, (\Delta \sin^2 \theta_W)_{\text{had}} = \left( \sum_{n=1}^N a_n Q^{2n} \right) / \left( 1 + \sum_{m=1}^M b_m Q^{2m} \right)$$

## Comparison at low $Q^2$



Note:  $(\Delta \sin^2 \theta_W)_{\text{had}}(-Q^2) \equiv (\Delta\alpha)_{\text{had}}(-Q^2) - (\Delta\alpha_2)_{\text{had}}(-Q^2)$

## Compute $(\Delta\alpha)_{\text{had}}^{(5)}(m_Z^2)$

**Method 1:** Dispersion relation (DR)

$$(\Delta\alpha)_{\text{had}}^{(5)}(Q^2) = -\frac{\alpha Q^2}{3\pi} P \int_{m_\pi^2}^{\infty} ds \frac{R(s)}{s(s-Q^2)} \leftarrow \text{for } Q^2 = m_Z^2$$

where for the  $R$ -ratio one uses the experimental data

$$R(Q^2) \equiv \frac{\sigma_{\text{total}}(e^+e^- \rightarrow \text{hadrons})}{\sigma(e^+e^- \rightarrow \mu^+\mu^-)}$$

up to certain energy, and then switches to perturbation theory.

**Method 2:** Adler function approach, aka "Euclidean split technique" [15, 16, 17, 18]

$$\begin{aligned}(\Delta\alpha)_{\text{had}}^{(5)}(m_Z^2) &= (\Delta\alpha)_{\text{had}}^{(5)}(-Q_0^2) \leftarrow \text{LQCD or DR for } Q^2 = -Q_0^2 \\ &+ \left( (\Delta\alpha)_{\text{had}}^{(5)}(-m_Z^2) - (\Delta\alpha)_{\text{had}}^{(5)}(-Q_0^2) \right) \leftarrow \text{pQCD or DR} \\ &+ \left( (\Delta\alpha)_{\text{had}}^{(5)}(m_Z^2) - (\Delta\alpha)_{\text{had}}^{(5)}(-m_Z^2) \right) \leftarrow \text{pQCD}\end{aligned}$$

# Compute $(\Delta\alpha)_{\text{had}}^{(5)}(m_Z^2)$

Mainz/CLS  $(\Delta\alpha)_{\text{had}}(m_Z^2) = 0.02773(15)$   
(lattice input + pQCD/Adler)

Jegerlehner 19  $(\Delta\alpha)_{\text{had}}(m_Z^2) = 0.02753(12)$   
( $R$ -ratio input + pQCD/Adler)

- ▶ The indirect determination of the Higgs mass is affected [2]:

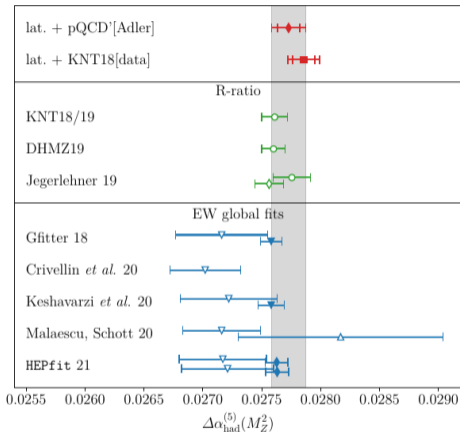
$$m_H = 91_{-16}^{+18} \text{ GeV} \rightarrow m_H = 78_{-?}^{+?} \text{ GeV}$$

- ▶ The agreement within errors at the  $Z$ -pole doesn't erase the tension for low  $Q^2$

▽ Leaving  $(\Delta\alpha)_{\text{had}}(m_Z^2)$  as a free parameter

△ Leaving  $(\Delta\alpha)_{\text{had}}(m_Z^2)$  and  $m_H$  as free parameters

▼ ◆ As ▽, but using priors for  $(\Delta\alpha)_{\text{had}}(m_Z^2)$  centred around the  $R$ -ratio/BMWc estimate



## Summary and Outlook

- ▶ Lattice+pQCD/Adler estimate for  $(\Delta\alpha)_{\text{had}}(m_Z^2)$  broadly agrees with global electroweak fits  $\rightarrow$  no contradiction with the Standard Model here
- ▶ Standard Model can accommodate a larger value for  $a_\mu$  without contradicting electroweak precision data
- ▶ Our result for  $a_\mu^{\text{win}}$ ,  $(\Delta\alpha)_{\text{had}}(-Q^2)$  and  $(\Delta\sin^2\theta_W)_{\text{had}}(-Q^2)$  are in tension with the  $R$ -ratio  $\rightarrow 3\sigma$  to  $5\sigma$

An update of the 2019 determination of  $a_\mu^{\text{HVP}}$  is ongoing:

- ▶ Investigate other time windows
- ▶ Reduce statistical errors
- ▶ Improve the scale setting
- ▶ Extend isospin breaking (IB) calculations to more ensembles

For a detailed explanation, see

- ▶ arXiv:2203.08676
- ▶ arXiv:2206.06582

## Lattice QCD

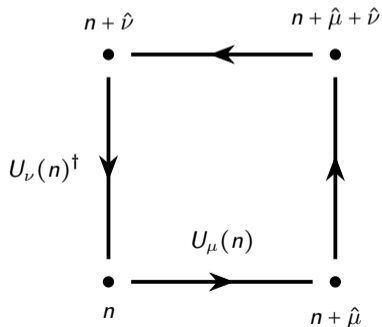
Replace the continuum space-time by a 4D Euclidean lattice

$$\Lambda = \{n = (n_1, n_2, n_3, n_4) \mid n_1, n_2, n_3, n_4 = 0, 1, \dots, N-1\}$$

Discretise the Euclidean action  $S$

Apply the **Feynman path integral** quantisation condition in Euclidean space

$$\langle O \rangle = \frac{1}{Z} \int \mathcal{D}[U] \mathcal{D}[\psi, \bar{\psi}] \exp(-S_F[\psi, \bar{\psi}, U] - S_G[U]) O[\psi, \bar{\psi}, U],$$



Integrate the fermion fields  $\psi$  and  $\bar{\psi}$  analytically, and the links  $U$  with importance sampling

$$\langle O \rangle = \frac{1}{N_{\text{cnfg}}} \sum_{\tau=1}^{N_{\text{cnfg}}} O[D^{-1}[U_\tau], U_\tau] + \mathcal{O}\left(\frac{1}{\sqrt{N_{\text{cnfg}}}}\right)$$

Use a **Markov process** to generate the links  $U_\tau$  according to the (positive) probability distribution density

$$W[U] = \frac{1}{Z} \mathcal{D}[U] \det[D_u D_d D_s \dots] \exp(-S_G[U])$$

## $\mathcal{O}(a)$ improved and renormalised vector currents

- Use the tensor current  $\Sigma_{\mu\nu}^a$  for  $\mathcal{O}(a)$  improvement [19, 20],

$$(V_k^a)_I^\alpha(x) = (V_k^a)^\alpha(x) + ac_V^\alpha(g_0)\tilde{\partial}_\nu\Sigma_{\mu\nu}^a(x), \quad \text{with } \alpha = L, C$$

- Renormalisation and mass-dependent improvement of local currents via [19, 20]

$$\begin{aligned} (V_k^3)_R^L &= Z_V (1 + 3\bar{b}_V am_q^{av} + b_V am_{q,l}) (V_k^3)_I^L, \\ \begin{pmatrix} V_k^8 \\ V_k^0 \end{pmatrix}_R^L &= Z_V \begin{pmatrix} 1 + 3\bar{b}_V am_q^{av} + \frac{b_V}{3}(am_{q,l} + 2am_{q,s}) & \left(\frac{b_V}{3} + f_V\right) \frac{2}{\sqrt{3}}(am_{q,l} - am_{q,s}) \\ \frac{r_V d_V}{3}(am_{q,l} - m_{q,s}) & r_V + r_V(3\bar{d}_V + d_V)am_q^{av} \end{pmatrix} \begin{pmatrix} V_k^8 \\ V_k^0 \end{pmatrix}_I^L \end{aligned}$$

- Two independent non-perturbative determinations of  $Z_V$ ,  $c_V^L$ ,  $c_V^C$ ,  $b_V$ ,  $\bar{b}_V$

Set 1 Large-volume CLS ensembles [19]

Set 2 Small-volume Schrödinger functional [21, 22] They differ by higher order cut-off effects.  $f_V$  is of  $\mathcal{O}(g_0^6)$  and unknown



## The $\Gamma$ method vs jackknife binning [23, 7]

Measurements are taken every 4 MDU.

Runs with the same trajectory length should show Langevin scaling,  $\bar{\tau}_{\bar{F}, \text{int}} \propto a^{-2}$ . OBC are taking to alleviate the increase in autocorrelations towards the The error estimate using the  $\Gamma$  method includes autocorrelations explicitly,

$$\left(\Delta_{\bar{F}}\right)^2 = 2\bar{\tau}_{F, \text{int}} \left(\Delta_0 \bar{F}\right)^2, \quad \left(\Delta_{\text{jack}} \bar{F}\right)^2 = \frac{N_B - 1}{N_B} \sum_{k=1}^{N_B} \left(f(c_\alpha^k) - \bar{F}\right)^2.$$

Both methods minimize the total error of the error to find the correct uncertainty,

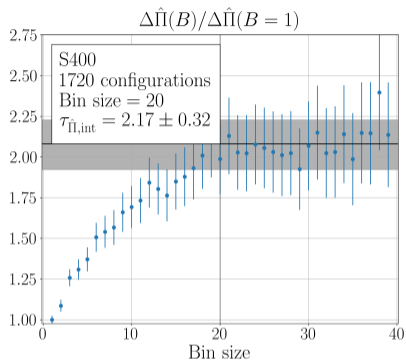
$$\frac{\Delta_{\text{total}} \left(\Delta_{\bar{F}}\right)}{\Delta_{\bar{F}}} \approx \frac{1}{2} \min_w \left( e^{-w/\tau_{F,D}} + 2\sqrt{\frac{w}{N}} \right), \quad \frac{\Delta_{\text{total}} \left(\Delta_{\text{jack}} \bar{F}\right)}{\Delta_{\text{jack}} \bar{F}} \approx \frac{1}{2} \min_B \left( \frac{\tau_{F,D}}{B} + \sqrt{\frac{2B}{N}} \right).$$

The systematic error of the error is different,

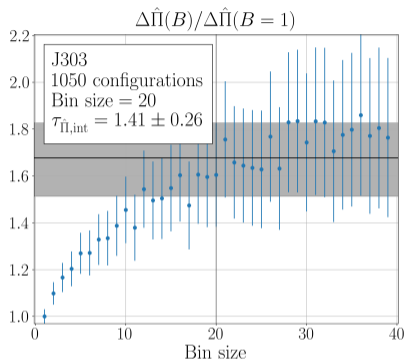
$$\frac{\Delta_{\text{sys}} \left(\Delta_{\bar{F}}\right)}{\Delta_{\text{sta}} \left(\Delta_{\bar{F}}\right)} \approx \frac{1}{\log(N/\tau_{F,D})}, \quad \frac{\Delta_{\text{sys}} \left(\Delta_{\text{jack}} \bar{F}\right)}{\Delta_{\text{sta}} \left(\Delta_{\text{jack}} \bar{F}\right)} = \frac{1}{2}.$$

The systematic error of the error for the  $\Gamma$  method vanishes with increasing statistics.

## The $\Gamma$ method vs jackknife binning [23]



Ensemble S400, with  $M_\pi = 351$  MeV



Ensemble J303, with  $M_\pi = 257$  MeV

The vertical line shows the estimated optimal bin size  $B$ , and the horizontal band shows

$$\Delta\bar{\Pi}(B)/\Delta\bar{\Pi}(1) = \sqrt{2\tau_{\bar{\Pi},\text{int}}} = \text{const},$$

which is the expected uncertainty increase when taking into account autocorrelations.

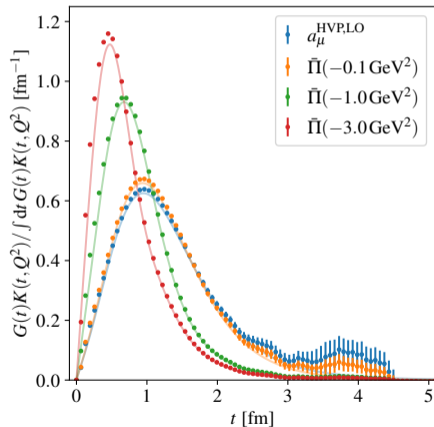
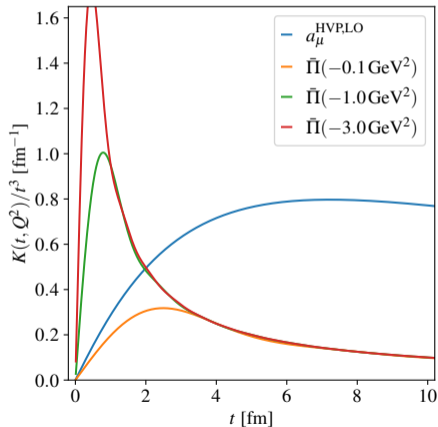
## The $\Gamma$ method vs jackknife binning

CLS	$aM_\pi$	Bin size	$\tau_{\bar{n},\text{int}}$
H101	0.1830 (5)	25	1.70 (26)
H102	0.1546 (5)	25	1.73 (27)
H105	0.1234 (13)	20	1.32 (27)
N101	0.1222 (5)	15	0.79 (11)
C101	0.0960 (6)	20	0.79 (10)
B450	0.1605 (4)	25	1.45 (24)
S400	0.1358 (4)	20	2.17 (32)
N451	0.1108 (3)	10	0.73 (10)
D450	0.0836 (4)	5	0.55 (7)
H200	0.1363 (5)	30	1.20 (19)
N202	0.1342 (3)	35	1.86 (45)
N203	0.1124 (2)	20	1.15 (17)
N200	0.0922 (3)	15	0.77 (10)
D200	0.0655 (3)	10	0.58 (6)
E250	0.0422 (2)	5	0.47 (4)
N300	0.1067 (3)	40	3.36 (67)
N302	0.0875 (3)	30	2.07 (33)
J303	0.0649 (2)	20	1.41 (26)
E300	0.0442 (1)	20	1.07 (22)

The pion masses were obtained by the Mainz group using an implementation of the PhD thesis [24].  $B$  and  $\tau_{\bar{n},\text{int}}$  are computed using the *Python* code [25].

## Time-momentum representation [3, 4]

$$K(t, Q^2) = t^2 - \frac{4}{Q^2} \sin^2 \left( \frac{Qt}{2} \right)$$



## Extrapolation to the physical point

Extrapolate to the isospin-symmetric physical point on the **dimensionless variables** [5, 2, 26]

$$a^2/8t_0^{\text{sym}} \rightarrow 0$$

$$\phi_2 = 8t_0 M_\pi^2 \rightarrow \phi_2^{\text{phy}} = 0.0806(17)$$

$$\phi_4 = 8t_0 (M_\pi^2/2 + M_k^2) \rightarrow \phi_4^{\text{phy}} = 1.124(24)$$

### Fit models

$$\bar{\pi}^{\text{charm}}(a^2/8t_0^{\text{sym}}, \phi_2) = \bar{\pi}^{\text{cc,sym}} + \delta_2^d (a^2/8t_0^{\text{sym}}) + \gamma_1^{\text{cc}} (\phi_2 - \phi_2^{\text{sym}})$$

$$\bar{\pi}^{08}(\phi_2, \phi_4) = \lambda_1 (\phi_4 - 3/2\phi_2)$$

$$\bar{\pi}^{i=33,88}(a^2/8t_0^{\text{sym}}, \phi_2, \phi_4) = \bar{\pi}^{\text{sym}} + \gamma_1^i (\phi_2 - \phi_2^{\text{sym}}) + \eta_1 (\phi_4 - \phi_4^{\text{sym}})$$

$$+ \gamma_2^i \left\{ \begin{array}{l} \log(\phi_2/\phi_2^{\text{sym}}) \\ (\phi_2 - \phi_2^{\text{sym}})^2 \end{array} \right\} + \left\{ \begin{array}{l} \delta_2^d (a^2/8t_0^{\text{sym}}) \\ \delta_2^d (a^2/8t_0^{\text{sym}}) + \delta_3^d (a^2/8t_0^{\text{sym}})^{3/2} \end{array} \right\}$$

## Total least-squares minimisation

We use the Levenberg-Marquardt algorithm [27] as implemented in the SciPy package [28] *least\_squares* routine. Different ensembles are uncorrelated,

$$\chi^2 = \sum_e \chi_e^2 \equiv \sum_e \begin{cases} \chi_{e,-}^2, & \text{if } M_{\pi,e} \neq M_{K,e}, \\ 1/2 (\chi_{e,33}^2 + \chi_{e,88}^2), & \text{if } M_{\pi,e} = M_{K,e}. \end{cases}$$

The index  $e$  runs over the ensembles.

$\chi_{e,-}^2$ ,  $\chi_{e,33}^2$  and  $\chi_{e,88}^2$  can be written with the same generic structure  $r^T \text{Cov}^{-1} r$ , where

$r = \text{model} - \text{data}$  is the vector of residues.

Cov is the covariance matrix, whose entries can be computed using

$$\text{Cov}_{e,.}[x, y] = \frac{1}{N_b - 1} \sum_{s=1}^{N_b} (x_s - E[x]) (y_s - E[y]),$$

where  $s$  runs over the bootstrap samples, of which there are  $N_b$  in total.

## $r$ and Cov for non-SU(3)<sub>f</sub>-symmetric ensembles

The residue vector is defined as

$$r_{e,-} = \begin{pmatrix} \phi_2 \\ \phi_4 \\ \bar{\Pi}(a, \phi_2, \phi_4; d=l, i=33) \\ \bar{\Pi}(a, \phi_2, \phi_4; d=s, i=33) \\ \bar{\Pi}(a, \phi_2, \phi_4; d=l, i=88) \\ \bar{\Pi}(a, \phi_2, \phi_4; d=s, i=88) \end{pmatrix} - \begin{pmatrix} \phi_2 \\ \phi_4 \\ \bar{\Pi}_{33}^l \\ \bar{\Pi}_{33}^s \\ \bar{\Pi}_{88}^l \\ \bar{\Pi}_{88}^s \end{pmatrix}_e,$$

where  $e$  runs over the ensembles data. The index structure of the covariance matrix is

$$\text{Cov}_{e,-} = \begin{pmatrix} \phi_2, \phi_2 & \phi_2, \phi_4 & \phi_2, \bar{\Pi}_{33}^l & \phi_2, \bar{\Pi}_{33}^s & \phi_2, \bar{\Pi}_{88}^l & \phi_2, \bar{\Pi}_{88}^s \\ \vdots & \phi_4, \phi_4 & \phi_4, \bar{\Pi}_{33}^l & \phi_4, \bar{\Pi}_{33}^s & \phi_4, \bar{\Pi}_{88}^l & \phi_4, \bar{\Pi}_{88}^s \\ \vdots & \vdots & \bar{\Pi}_{33}^l, \bar{\Pi}_{33}^l & \bar{\Pi}_{33}^l, \bar{\Pi}_{33}^s & \bar{\Pi}_{33}^l, \bar{\Pi}_{88}^l & \bar{\Pi}_{33}^l, \bar{\Pi}_{88}^s \\ \vdots & \vdots & \vdots & \bar{\Pi}_{33}^s, \bar{\Pi}_{33}^s & \bar{\Pi}_{33}^s, \bar{\Pi}_{88}^l & \bar{\Pi}_{33}^s, \bar{\Pi}_{88}^s \\ \vdots & \vdots & \vdots & \vdots & \bar{\Pi}_{88}^l, \bar{\Pi}_{88}^l & \bar{\Pi}_{88}^l, \bar{\Pi}_{88}^s \\ \dots & \dots & \dots & \dots & \dots & \bar{\Pi}_{88}^s, \bar{\Pi}_{88}^s \end{pmatrix}_e$$

## $r$ and Cov for $SU(3)_f$ -symmetric ensembles

The residue vector is defined as

$$r_{e,i} = \begin{pmatrix} \phi_2 \\ \bar{\Pi}(a, \phi_2, 3\phi_2/2; d = l, i) \\ \bar{\Pi}(a, \phi_2, 3\phi_2/2; d = s, i) \end{pmatrix} - \begin{pmatrix} \phi_2 \\ \bar{\Pi}_i^l \\ \bar{\Pi}_i^s \end{pmatrix}_e,$$

where  $e$  runs over the ensembles data. The index structure of the covariance matrix is

$$\text{Cov}_{e,i} = \begin{pmatrix} \phi_2, \phi_2 & \phi_2, \bar{\Pi}_i^l & \phi_2, \bar{\Pi}_i^s \\ \vdots & \bar{\Pi}_i^l, \bar{\Pi}_i^l & \bar{\Pi}_i^l, \bar{\Pi}_i^s \\ \dots & \dots & \bar{\Pi}_i^s, \bar{\Pi}_i^s \end{pmatrix}_e$$



## Jacobian

We define a vector  $y$  of length  $m \times 1$  containing all the fit parameters,

$$y \equiv (\bar{\Pi}^{\text{sym}}, \alpha_{2,S}, \alpha_{3,S}, \beta_{1,33}, \text{ etc.})$$

The vector  $y$  includes  $\phi_2$  for the  $SU(3)_f$ -symmetric ensembles, and  $\phi_2$  and  $\phi_4$  for the rest. Then, we apply the Cholesky decomposition on  $\chi_{e,-}^2, \chi_{e,33}^2, \chi_{e,88}^2$ ,

$$\chi_{e,.} = L_{e,.}^{-1} r_{e,.},$$

such that  $\chi_{e,.}$  is a  $n \times 1$  vector, with  $n$  the number of dependent ( $\bar{\Pi}$ ) plus independent ( $\phi_2, \phi_4$ ) variables for a given ensemble.

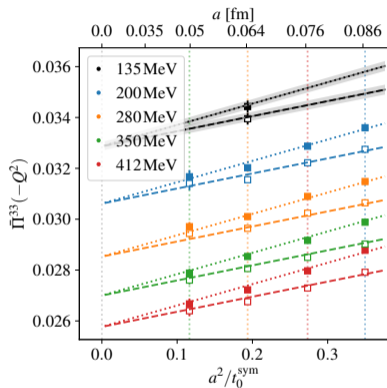
Then, we compute the  $m \times n$  matrix of derivatives

$$\left( \frac{\partial \chi_{e,.}}{\partial y} \right)^T = L_{e,.}^{-1} \left( \frac{\partial r_{e,.}}{\partial y} \right)^T,$$

For  $SU(3)_f$ -symmetric ensembles,  $m = 10$  and  $n = 3$ , while  $m = 11$  and  $n = 6$  for the rest. Then, the Jacobian for every ensemble is [29]

$$\frac{\partial \chi_e}{\partial y} \chi_e = \begin{cases} \frac{\partial \chi_{e,-}}{\partial y} \chi_{e,-}, & \text{if } M_{\pi,e} \neq M_{K,e} \\ \frac{1}{2} \left( \frac{\partial \chi_{e,33}}{\partial y} \chi_{e,33} + \frac{\partial \chi_{e,88}}{\partial y} \chi_{e,88} \right), & \text{if } M_{\pi,e} = M_{K,e}. \end{cases}$$

## Lattice spacing dependence

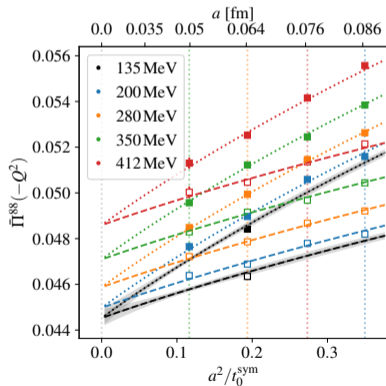


Smooth step function between  $a^2$  and  $a^2 + a^3$

$$\Theta(Q^2) = 0.5 \left( 1 + \tanh\left(\frac{Q^2 - 2.5 \text{ GeV}^2}{1.0 \text{ GeV}^2}\right) \right)$$

Logarithmic corrections to the  $a^2$  behaviour [30]

$$\tilde{c}_{\bar{\Pi}}(Q^2) \cdot (a^2/t_0^{\text{sym}}) \log(t_0^{\text{sym}}/a^2)/2 \sim 0$$



## Scale-setting uncertainty

Dominant uncertainty for  $0 < Q^2 \lesssim 3 \text{ GeV}^2$

Although  $\bar{\Pi}$  is dimensionless, the scale enters indirectly through

The virtuality  $8t_0 Q^2$  in the kernel  $K(t, Q^2)$  of the TMR

The physical point definition  $\phi_2^{\text{phy}}, \phi_4^{\text{phy}}$

Using linear error propagation, the relative error of  $\bar{\Pi}$  is

$$\frac{\Delta \bar{\Pi}}{\bar{\Pi}} \approx \left| \frac{2l_0^2 Q^2}{\bar{\Pi}} \frac{\partial \bar{\Pi}}{\partial l_0^2 Q^2} + \frac{2\phi_2^{\text{phy}}}{\bar{\Pi}} \frac{\partial \bar{\Pi}}{\partial \phi_2^{\text{phy}}} + \frac{2\phi_4^{\text{phy}}}{\bar{\Pi}} \frac{\partial \bar{\Pi}}{\partial \phi_4^{\text{phy}}} \right| \frac{\Delta l_0}{l_0}$$

The first term is positive, and varies with  $Q^2$

The second and third terms are negative

$\Delta \bar{\Pi} / \bar{\Pi} \sim 0$  in some cases

} → We use bootstrap sampling instead

Scale setting:  $l_0 \equiv \sqrt{8t_0} = 0.415 \text{ (4) (2) fm [5]}$

Improved determination in progress

## Isospin breaking effects [34, 24, 35]

Evaluate quark-connected  $\bar{\Pi}$  in QCD + QED at  $M_\pi \sim 220$  MeV  $\rightarrow$  Estimate relative size of isospin breaking effects

$\rightarrow$  Add to error budget

$\rightarrow$  Non-compact QED<sub>L</sub>-action for IR regularisation, Coulomb gauge [31]

$\rightarrow$  Same boundary conditions for the photon and gluon fields

$\rightarrow$  Reweighting and leading perturbative expansion in  $\Delta\epsilon = \epsilon - \epsilon^{(0)}$  around  $\epsilon^{(0)}$ , where

QCD + QED parametrised by  $\epsilon = (M_u, M_d, M_s, \beta, e^2)$

QCD<sub>iso</sub> parametrised by  $\epsilon^{(0)} = (M_{ud}^{(0)}, M_{ud}^{(0)}, M_s^{(0)}, \beta^{(0)}, 0)$

[32, 33]

$\rightarrow$  Neglect IB effects in the scale

$\rightarrow$  Renormalisation scheme: Match QCD + QED and QCD<sub>iso</sub> using

$$M_{\pi^0}^2 \propto M_u + M_d$$

$$M_{K^+}^2 - M_{K^0}^2 - M_{\pi^+}^2 + M_{\pi^0}^2 \propto M_u - M_d$$

$$M_{K^+}^2 + M_{K^0}^2 - M_{\pi^+}^2 \propto M_s$$

## Missing quark contributions

The charm-quark contribution is determined from the quark-connected component alone. Therefore, there are two missing effects:

### → Valence charm-quark loops

[9] reports this contribution to be  $< 1\%$  of the  $u, d, s$  quark-disconnected contribution to  $a_\mu^{\text{HVP}}$  → **0.1‰ effect we neglect**

### → Sea charm-quark loops

To estimate the effect of quenching, we employ a phenomenological estimate,

Split  $\bar{\Pi}$  into two parts,

$$\bar{\Pi}(-Q_0^2) = \underbrace{[\bar{\Pi}(-Q_0^2) - \bar{\Pi}(-1 \text{ GeV}^2)]}_{\textcircled{1}} + \underbrace{\bar{\Pi}(-1 \text{ GeV}^2)}_{\textcircled{2}}$$

① Charm sea-quark effects appear at  $\mathcal{O}(\alpha_s^2)$  in perturbation theory → **negligible**

②  $D^+ D^-, D^0 \bar{D}^0, D_s^+ D_s^-$  contribute to the  $(u, d, s)$  vector correlators.  
Using scalar-QED → **3‰ effect added to error budget**

The bottom-quark contribution is determined by [8] → **maximum 3‰ effect added to error budget to compare with phenomenology**

## Relating $\bar{\Pi}$ and the Stieltjes function

The integral representation of a Stieltjes function  $\Phi(z)$  is [36, 37],

$$\Phi(z) = \int_0^{1/R} \frac{d\nu(\tau)}{1 + \tau z},$$

where  $\nu(z)$  is real, bounded, non-decreasing on the interval  $[0, 1/R]$ , and takes infinitely many values on that said interval.  $\Phi(z)$  is analytic in the entire complex plane except on the cut  $z \in (-\infty, -R]$ , and decreases monotonically in the range  $z \in (-R, \infty)$ . Choosing [37]

$$\tau = \frac{1}{s},$$

$$R = 4M_\pi^2,$$

$$d\nu(\tau) = d\tau \rho(1/\tau),$$

$$\rho(1/\tau) = \frac{1}{\pi} \text{Im}\Pi(1/\tau),$$

we see that  $\bar{\Pi}$  is a Stieltjes function [37],

$$\bar{\Pi}(-Q^2) = Q^2 \Phi(Q^2),$$

$$\Phi(Q^2) = \int_{4M_\pi^2}^{\infty} ds \frac{\rho(s)}{s(s + Q^2)}.$$

The spectral function  $\rho(s)$  is non-negative in the integration range.

## Relating the Stieltjes function and the Padé approximants (PAs)

A Padé approximant  $R_M^N(Q^2)$  is the ratio of two polynomials of degrees N and M [38],

$$R_M^N(Q^2) = \frac{\sum_{n=0}^N a_n Q^{2n}}{1 + \sum_{m=1}^M b_m Q^{2m}}$$

To build Padé approximants (PAs) to describe  $\Phi(Q^2)$ , we employ the following theorem [38, 39]: Given P points  $(Q_i^2, \Phi(Q_i^2))$ ,  $i \in \{1, \dots, P\}$ , a sequence of Padé approximants can be constructed converging to  $\Phi(Q^2)$  in the limit  $P \rightarrow \infty$  on any closed, bounded region of the complex plane, excluding the cut  $Q^2 \in (-\infty, -4M_\pi^2]$ . Then, the Stieltjes function  $\Phi(Q^2)$  can be built as a continued fraction [38],

$$\Phi(Q^2) = \frac{\psi_1(Q_1^2)}{1 + \frac{(Q^2 - Q_1^2) \psi_2(Q_2^2)}{1 + \frac{(Q^2 - Q_2^2) \psi_3(Q_3^2)}{\dots 1 + (Q^2 - Q_{P-1}^2) \psi_P(Q_P^2)}}}$$

The functions  $\psi_i$  can be constructed recursively using [40]

$$\psi_1 = \Phi(Q_1^2), \quad \psi_i(Q^2) = \frac{\psi_{i-1}(Q_{i-1}^2) - \psi_{i-1}(Q_i^2)}{(Q^2 - Q_{i-1}^2) \psi_{i-1}(Q^2)}, \quad i > 1.$$

## Inputs to the Adler function approach

**First term:** Lattice result for  $(\Delta\alpha)_{\text{had}}^{(5)}(-Q_0^2)$  for  $Q_0^2 = 3$  to  $7 \text{ GeV}^2$

**Second term:** The Adler function

$$D(-Q^2) = \frac{3\pi}{\alpha} Q^2 \frac{d(\Delta\alpha)_{\text{had}}^{(5)}(Q^2)}{dQ^2}$$

It is known to three loops in pQCD  $\rightarrow$  Jegerlehner's **pQCDAdler** package

$$\left[ (\Delta\alpha)_{\text{had}}^{(5)}(-m_Z^2) - (\Delta\alpha)_{\text{had}}^{(5)}(-Q_0^2) \right]_{\text{pQCD/Adler}} = \frac{\alpha}{3\pi} \int_{Q_0^2}^{m_Z^2} \frac{dQ^2}{Q^2} D(Q^2)$$

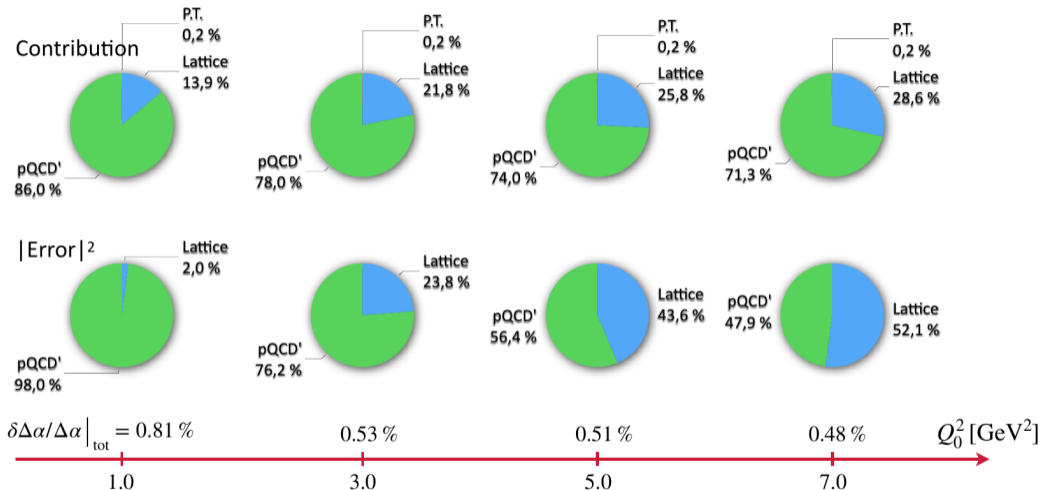
The result depends on  $Q_0^2$

**Third term:** Perturbation theory [41]

$$\left[ (\Delta\alpha)_{\text{had}}^{(5)}(m_Z^2) - (\Delta\alpha)_{\text{had}}^{(5)}(-m_Z^2) \right]_{\text{pQCD}} = 0.000\,045(2)$$



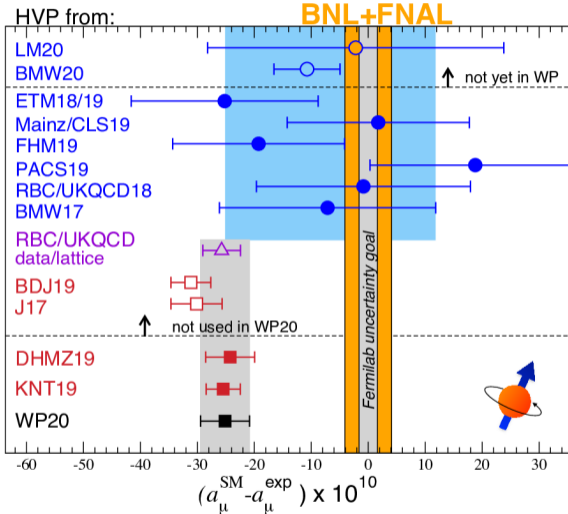
# Relative contributions to $(\Delta\alpha)_{\text{had}}^{(5)}(m_Z^2)$



Slide taken from Hartmut Wittig's Lattice 2022 talk

Teseo San José

# The hadronic vacuum polarisation contribution to the muon $g - 2$



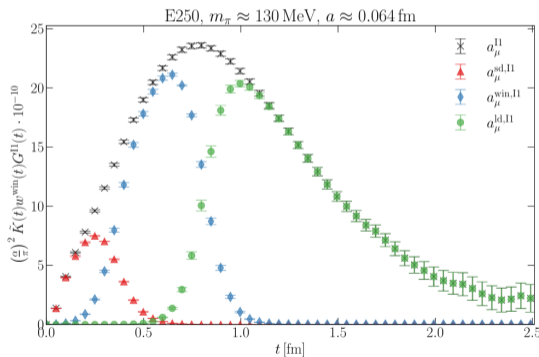
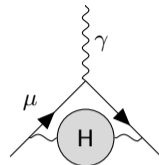
←  $a_\mu^{\text{HVP}}$  status [42]

- BMW20 prediction [43] has similar precision to phenomenology, but it deviates from data-driven results
- We need more precise lattice determinations. Challenging systematics:
  - ▶ At short distances, cut-off effects
  - ▶ At long distances, noise
- For a clear comparison between lattice determinations → Use time windows in the TMR as benchmarks [44]

# The time-momentum representation (TMR) for $a_\mu^{\text{HVP}}$

Intermediate Euclidean time window of  $a_\mu^{\text{HVP}}$ :

$$a_\mu^{\text{win}} \equiv \left(\frac{\alpha}{\pi}\right)^2 \int_0^\infty dt \tilde{K}(t) G^{\gamma\gamma}(t) [\Theta(t, t_0, \Delta) - \Theta(t, t_1, \Delta)]$$



$$G^{\gamma\gamma}(t) = -\frac{a^3}{3} \sum_{k=1}^3 \sum_{\vec{x}} \langle V_k^\gamma(\vec{x}) V_k^\gamma(0) \rangle_{\text{QCD}}$$

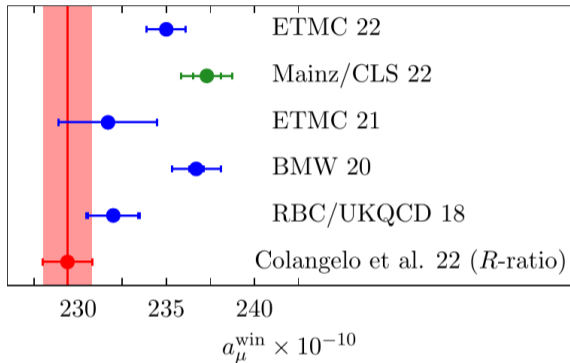
$$\Theta(t, t', \Delta) \equiv \frac{1}{2} (1 + \tanh[(t - t')/\Delta])$$

$$t_0 = 0.4 \text{ fm}, \quad t_1 = 1.0 \text{ fm}, \quad \Delta = 0.15 \text{ fm}$$

Intermediate window:

- ▶ Cut-off effects are suppressed
- ▶ No noise problem
- ▶ Per-mil uncertainty

## Comparing $a_\mu^{\text{win}}$ with the $R$ -ratio



- 3.9  $\sigma$  tension with data-driven estimate [45]
- Need to look at the other windows

- [1] P. A. Zyla et al. "Review of Particle Physics". In: *PTEP* 2020.8 (2020), p. 083C01. DOI: 10.1093/ptep/ptaa104.
- [2] R. L. Workman et al. "Review of Particle Physics". In: *PTEP* 2022 (2022), p. 083C01. DOI: 10.1093/ptep/ptac097.
- [3] D. Bernecker and H. B. Meyer. "Vector correlators in lattice QCD: Methods and applications". In: *European Physical Journal A* 47, 148 (Nov. 2011), p. 148. DOI: 10.1140/epja/i2011-11148-6. arXiv: 1107.4388 [hep-lat].
- [4] A. Francis et al. "New representation of the Adler function for lattice QCD". In: *prd* 88.5, 054502 (Sept. 2013), p. 054502. DOI: 10.1103/PhysRevD.88.054502. arXiv: 1306.2532 [hep-lat].
- [5] Mattia Bruno, Tomasz Korzec, and Stefan Schaefer. "Setting the scale for the CLS 2 + 1 flavor ensembles". In: *Phys. Rev. D* 95.7 (2017), p. 074504. DOI: 10.1103/PhysRevD.95.074504. arXiv: 1608.08900 [hep-lat].
- [6] Antoine Gérardin et al. "The leading hadronic contribution to  $(g - 2)_\mu$  from lattice QCD with  $N_f = 2 + 1$  flavours of  $O(a)$  improved Wilson quarks". In: *Phys. Rev. D* 100.1 (2019), p. 014510. DOI: 10.1103/PhysRevD.100.014510. arXiv: 1904.03120 [hep-lat].
- [7] Mattia Bruno et al. "Simulation of QCD with  $N_f = 2 + 1$  flavors of non-perturbatively improved Wilson fermions". In: *JHEP* 02 (2015), p. 043. DOI: 10.1007/JHEP02(2015)043. arXiv: 1411.3982 [hep-lat].
- [8] B. Colquhoun et al. " $\Upsilon$  and  $\Upsilon'$  Leptonic Widths,  $a_\mu^b$  and  $m_b$  from full lattice QCD". In: *Phys. Rev. D* 91.7 (2015), p. 074514. DOI: 10.1103/PhysRevD.91.074514. arXiv: 1408.5768 [hep-lat].

- [9] Sz. Borsanyi et al. “Hadronic vacuum polarization contribution to the anomalous magnetic moments of leptons from first principles”. In: *Phys. Rev. Lett.* 121.2 (2018), p. 022002. DOI: 10.1103/PhysRevLett.121.022002. arXiv: 1711.04980 [hep-lat].
- [10] Maxwell T. Hansen and Agostino Patella. “Finite-volume and thermal effects in the leading-HVP contribution to muonic  $(g - 2)$ ”. In: *JHEP* 2010.10 (Oct. 2020), p. 029. DOI: 10.1007/jhep10(2020)029. arXiv: 2004.03935 [hep-lat].
- [11] Maxwell T. Hansen and Agostino Patella. “Finite-volume effects in  $(g - 2)_{\mu}^{\text{HVP,LO}}$ ”. In: *Phys. Rev. Lett.* 123 (2019), p. 172001. DOI: 10.1103/PhysRevLett.123.172001. arXiv: 1904.10010 [hep-lat].
- [12] Meyer. “Lattice QCD and the Timelike Pion Form Factor”. In: *Phys. Rev. Lett.* 107 (2011), p. 072002. DOI: 10.1103/PhysRevLett.107.072002. arXiv: 1105.1892 [hep-lat].
- [13] M. Della Morte et al. “The hadronic vacuum polarization contribution to the muon  $g - 2$  from lattice QCD”. In: *ArXiv e-prints* (May 2017). arXiv: 1705.01775 [hep-lat].
- [14] Laurent Lellouch and Martin Luscher. “Weak transition matrix elements from finite volume correlation functions”. In: *Commun. Math. Phys.* 219 (2001), pp. 31–44. DOI: 10.1007/s002200100410. arXiv: hep-lat/0003023.
- [15] K. G. Chetyrkin, Johann H. Kuhn, and M. Steinhauser. “Three loop polarization function and  $O(\alpha_s^2)$  corrections to the production of heavy quarks”. In: *Nucl. Phys. B* 482 (1996), pp. 213–240. DOI: 10.1016/S0550-3213(96)00534-2. arXiv: hep-ph/9606230.

- [16] S. Eidelman et al. “Testing nonperturbative strong interaction effects via the Adler function”. In: *Phys. Lett. B* 454 (1999), pp. 369–380. DOI: 10.1016/S0370-2693(99)00389-5. arXiv: hep-ph/9812521.
- [17] F. Jegerlehner. “Hadronic effects in  $(g - 2)(\mu)$  and  $\alpha(\text{QED})(M(Z))$ : Status and perspectives”. In: *4th International Symposium on Radiative Corrections: Applications of Quantum Field Theory to Phenomenology*. Jan. 1999, pp. 75–89. arXiv: hep-ph/9901386.
- [18] F. Jegerlehner. “The Running fine structure constant  $\alpha(E)$  via the Adler function”. In: *Nucl. Phys. B Proc. Suppl.* 181-182 (2008). Ed. by Cesare Bini and Graziano Venanzoni, pp. 135–140. DOI: 10.1016/j.nuclphysbps.2008.09.010. arXiv: 0807.4206 [hep-ph].
- [19] Antoine Gerardin, Tim Harris, and Harvey B. Meyer. “Nonperturbative renormalization and  $O(a)$ -improvement of the nonsinglet vector current with  $N_f = 2 + 1$  Wilson fermions and tree-level Symanzik improved gauge action”. In: *Phys. Rev. D* 99.1 (2019), p. 014519. DOI: 10.1103/PhysRevD.99.014519. arXiv: 1811.08209 [hep-lat].
- [20] Marco Cè et al. “The hadronic running of the electromagnetic coupling and the electroweak mixing angle from lattice QCD”. In: *JHEP* 08 (2022), p. 220. DOI: 10.1007/JHEP08(2022)220. arXiv: 2203.08676 [hep-lat].
- [21] Jochen Heitger and Fabian Joswig. “The renormalised  $O(a)$  improved vector current in three-flavour lattice QCD with Wilson quarks”. In: *Eur. Phys. J. C* 81.3 (2021), p. 254. DOI: 10.1140/epjc/s10052-021-09037-4. arXiv: 2010.09539 [hep-lat].

- [22] Patrick Fritzsche. “Mass-improvement of the vector current in three-flavor QCD”. In: *JHEP* 06 (2018), p. 015. DOI: 10.1007/JHEP06(2018)015. arXiv: 1805.07401 [hep-lat].
- [23] Ulli Wolff. “Monte Carlo errors with less errors”. In: *Comput. Phys. Commun.* 156 (2004). [Erratum: *Comput.Phys.Commun.* 176, 383 (2007)], pp. 143–153. DOI: 10.1016/S0010-4655(03)00467-3. arXiv: hep-lat/0306017.
- [24] Andreas Risch. “Isospin breaking effects in hadronic matrix elements on the lattice”. eng. PhD thesis. Mainz, 2021. DOI: <http://doi.org/10.25358/openscience-6314>.
- [25] Barbara De Palma et al. “A Python program for the implementation of the  $\Gamma$ -method for Monte Carlo simulations”. In: *Comput. Phys. Commun.* 234 (2019), pp. 294–301. DOI: 10.1016/j.cpc.2018.07.004. arXiv: 1703.02766 [hep-lat].
- [26] T. Blum et al. *Discussion: criteria for inclusion in WP update at the last g-2 theory initiative workshop, Wed 30/06 at 15:05 CEST. 2021.* URL: <https://agenda.hepl.phys.nagoya-u.ac.jp/indico/conferenceDisplay.py?ovw=True&confId=1691>.
- [27] Ananth Ranganathan. “The levenberg-marquardt algorithm”. In: *Tutorial on LM algorithm* 11.1 (2004), pp. 101–110.
- [28] Pauli Virtanen et al. “SciPy 1.0: Fundamental Algorithms for Scientific Computing in Python”. In: *Nature Methods* 17 (2020), pp. 261–272. DOI: 10.1038/s41592-019-0686-2.
- [29] Darrell A. Turkington. “New Matrix Calculus Results”. In: *Generalized Vectorization, Cross-Products, and Matrix Calculus*. Cambridge University Press, 2013, pp. 164–213. DOI: 10.1017/CB09781139424400.006.



- [30] Marco Cè et al. “Vacuum correlators at short distances from lattice QCD”. In: (June 2021). arXiv: 2106.15293 [hep-lat].
- [31] Masashi Hayakawa and Shunpei Uno. “QED in finite volume and finite size scaling effect on electromagnetic properties of hadrons”. In: *Prog. Theor. Phys.* 120 (2008), pp. 413–441. DOI: 10.1143/PTP.120.413. arXiv: 0804.2044 [hep-ph].
- [32] G. M. de Divitiis et al. “Isospin breaking effects due to the up-down mass difference in Lattice QCD”. In: *JHEP* 04 (2012), p. 124. DOI: 10.1007/JHEP04(2012)124. arXiv: 1110.6294 [hep-lat].
- [33] G. M. de Divitiis et al. “Leading isospin breaking effects on the lattice”. In: *Phys. Rev. D* 87.11 (2013), p. 114505. DOI: 10.1103/PhysRevD.87.114505. arXiv: 1303.4896 [hep-lat].
- [34] Andreas Risch and Hartmut Wittig. “Leading isospin breaking effects in the HVP contribution to  $a_\mu$  and to the running of  $\alpha$ ”. In: *PoS LATTICE2021* (2022), p. 106. DOI: 10.22323/1.396.0106. arXiv: 2112.00878 [hep-lat].
- [35] Andreas Risch and Hartmut Wittig. “Leading isospin breaking effects in the hadronic vacuum polarisation with open boundaries”. In: *PoS LATTICE2019* (2019), p. 296. DOI: 10.22323/1.363.0296. arXiv: 1911.04230 [hep-lat].
- [36] Jacques Hadamard. *Essai sur l'étude des fonctions, données par leur développement de Taylor*. Gauthier-Villars, 1892.

- [37] Christopher Aubin et al. “Model-independent parametrization of the hadronic vacuum polarization and  $g-2$  for the muon on the lattice”. In: *Phys. Rev. D* 86 (2012), p. 054509. DOI: 10.1103/PhysRevD.86.054509. arXiv: 1205.3695 [hep-lat].
- [38] Michael Barnsley. “The bounding properties of the multipoint Padé approximant to a series of Stieltjes on the real line”. In: *Journal of Mathematical Physics* 14.3 (1973), pp. 299–313. DOI: 10.1063/1.1666314. eprint: <https://doi.org/10.1063/1.1666314>. URL: <https://doi.org/10.1063/1.1666314>.
- [39] George A. Baker. “Best Error Bounds for Padé Approximants to Convergent Series of Stieltjes”. In: *Journal of Mathematical Physics* 10.5 (1969), pp. 814–820. DOI: 10.1063/1.1664911. eprint: <https://doi.org/10.1063/1.1664911>. URL: <https://doi.org/10.1063/1.1664911>.
- [40] G. A. Baker. “Best error bounds for pade approximants to convergent series of stieltjes”. In: *J. Math. Phys.* 10 (1969), pp. 814–820. DOI: 10.1063/1.1664911.
- [41] F. Jegerlehner. “ $\alpha_{QED,eff}(s)$  for precision physics at the FCC-ee/ILC”. In: *CERN Yellow Reports: Monographs* 3 (2020). Ed. by A. Blondel et al., pp. 9–37. DOI: 10.23731/CYRM-2020-003.9.
- [42] G. Colangelo et al. “Prospects for precise predictions of  $a_\mu$  in the Standard Model”. In: (Mar. 2022). arXiv: 2203.15810 [hep-ph].
- [43] Sz. Borsanyi et al. “Leading hadronic contribution to the muon magnetic moment from lattice QCD”. In: *Nature* 593.7857 (2021), pp. 51–55. DOI: 10.1038/s41586-021-03418-1. arXiv: 2002.12347 [hep-lat].

- [44] T. Blum et al. “Calculation of the hadronic vacuum polarization contribution to the muon anomalous magnetic moment”. In: *Phys. Rev. Lett.* 121.2 (2018), p. 022003. DOI: 10.1103/PhysRevLett.121.022003. arXiv: 1801.07224 [hep-lat].
- [45] G. Colangelo et al. “Data-driven evaluations of Euclidean windows to scrutinize hadronic vacuum polarization”. In: *Phys. Lett. B* 833 (2022), p. 137313. DOI: 10.1016/j.physletb.2022.137313. arXiv: 2205.12963 [hep-ph].